Chemical Science

ROYAL SOCIETY OF CHEMISTRY

EDGE ARTICLE

View Article Online
View Journal | View Issue

Cite this: *Chem. Sci.*, 2021, **12**, 2209

All publication charges for this article have been paid for by the Royal Society of Chemistry

Received 28th November 2020
Accepted 15th December 2020

DOI: 10.1039/d0sc06529c

rsc.li/chemical-science

Iridium-promoted deoxyglycoside synthesis: stereoselectivity and mechanistic insight†

Kumar Bhaskar Pal,[ab] Aoxin Guo,[b] Mrinmoy Das,[b] Jiande Lee,[bc] Gábor Báti,[b] Benjamin Rui Peng Yip,[b] Teck-Peng Loh[abd] and Xue-Wei Liu*[b]

Herein, we devised a method for stereoselective *O*-glycosylation using an Ir(I)-catalyst which enables both hydroalkoxylation and nucleophilic substitution of glycals with varying substituents at the C3 position. In this transformation, 2-deoxy-α-*O*-glycosides were acquired when glycals equipped with a notoriously poor leaving group at C3 were used; in contrast 2,3-unsaturated-α-*O*-glycosides were produced from glycals that bear a good leaving group at C3. Mechanistic studies indicate that both reactions proceed *via* the directing mechanism, through which the acceptor coordinates to the Ir(I) metal in the α-face-coordinated Ir(I)-glycal π-complex and then attacks the glycal that contains the *O*-glycosidic bond in a *syn*-addition manner. This protocol exhibits good functional group tolerance and is exemplified with the preparation of a library of oligosaccharides in moderate to high yields and with excellent stereoselectivities.

Introduction

Deoxy sugars, constituting essential structural components in a variety of biologically active natural products, have drawn significant attention from carbohydrate chemists lately.[1] Over the past few years, acid and base promoted synthesis of 2-deoxy sugars has become popular in the field of carbohydrate chemistry.[2] However, glycosylation by these approaches is often conducted at either low or high temperatures, with the possibility of obtaining appreciable amounts of unwanted hemiacetal side products.[2b,c,e,3] In comparison, transition metal catalyzed glycosylation with glycals, compatible with acid and base-labile substrates and amenable to moderate conditions, promises improved alternatives to the conventional methods. During recent years, transition metals have played an important role in the chemical synthesis of oligosaccharides, with a flow of intriguing glycosylation methodologies involving a variety of transition metal catalysts reported.[4–16] Conceptually, by installing specific substituents onto the donors[6] and/or control of the oxidation state of the transition metal in the catalysts, face-selective coordination of the catalytic metal complex with the olefinic pyranose ring can be feasibly achieved,[7] enabling stereoselective construction of glycosidic linkages. Additionally, glycal donors can be activated with a catalytic amount of the transition metal catalyst, while in conventional acid or base promoted glycosylation reactions, saturated glycosyl donors consume stoichiometric amounts of activating agents.

An important class of transition metal catalyzed glycosylation methodologies are those which exploit palladium catalysts for stereoselective synthesis of 2,3-unsaturated and 2-deoxy glycosides from glycals under anhydrous reaction conditions to preclude formation of the hydrolyzed products.[7,8] Nevertheless, to access different types of glycoside structures, glycosylation of glycals requires different Pd-catalytic systems with various phosphine ligands. And with certain Pd-catalysts, chemoselectivity is achieved by conducting the reaction at varying temperatures.[7,8] Analogous to the established palladium catalysts, iridium complexes have been well known to be efficient catalysts for allylic substitution reactions[9] and hydro-functionalisation[10] of olefins, while the aptness of iridium catalysts for glycosylation has scarcely been explored. Though Nishimura *et al.*[17] reported a pioneering iridium-catalyzed stereoselective *C*-glycosylation of glycals *via* C–H activation of arenes, no iridium-catalyzed-*O*-glycosylation with direct activation of glycal scaffolds has been reported to date.

Inspired by the success of Pd-catalyzed glycosylation methodologies and advancements in the development of Ir(I)-catalysts towards allylic addition and substitution reactions and as a part of our continuing effort in exploring the advanced stereo-

[a]*Institute of Advanced Synthesis, Northwestern Polytechnical University, Xi'an 710072, China*

[b]*Division of Chemistry and Biological Chemistry, School of Physical and Mathematical Sciences, Nanyang Technological University, 21 Nanyang Link, Singapore 637371. E-mail: xuewei@ntu.edu.sg*

[c]*Nanyang Environment and Water Research Institute, Nanyang Technological University, 1 Cleantech Loop, Singapore 637141*

[d]*Yangtze River Delta Research Institute of Northwestern Polytechnical University, Taicang Jiangsu, 215400, China*

† Electronic supplementary information (ESI) available. See DOI: 10.1039/d0sc06529c

and regioselective glycosylation, we envisioned that Ir-catalyzed chemistry can be applied to the olefinic glycal substrates to achieve stereoselective *O*-glycosylation. In this article, we describe novel ligand free iridium-catalyzed *O*-glycosylation that enables substrate-controlled access to both 2-deoxy glycosides and 2,3-unsaturated glycosides from easily accessible protected glycals at room temperature, with exclusive α-stereoselectivity (Scheme 1).

Results and discussion

Our attempt commenced with the screening of catalysts employing 3,4,6-tri-*O*-benzyl-D-galactal (**1a**) as the glycosyl donor and 1,2:3,4-di-*O*-isopropylidene-α-D-galactopyranose (**2a**) as the model glycosyl acceptor (Table 1). Not a trace of the 2-deoxy-*O*-glycoside was detected when 3.5 mol% $[Ir(COD)Cl]_2$ was used as the catalyst. It provided the desired 2-deoxyglycoside (**3a**) with the addition of $[Ir(COD)Cl]_2$/AgOTf and, to our satisfaction, the yield of the reaction was improved significantly to 77% with 10.5 mol% loading of AgOTf in CH_2Cl_2 (Table 1, entry 4). Screening of the silver salts implied that the *O*-glycosylation occurred most efficiently in the presence of AgOTf (10.5 mol%). While assessing the solvents, we found that the reaction didn't proceed in 1,4-dioxane; however, the use of MeCN, toluene, DCE and $CHCl_3$ as solvents provided 27%, 41%, 52% and 66% yields of the desired 2-deoxyglycoside, respectively, but they turned out to be less effective compared to CH_2Cl_2 (Table 1). It is noteworthy that not a trace of the desired glycosylated product was observed with the bulky $P(OPh)_3$ ligand, possibly due to the obstruction of the nucleophile acceptor from approaching the glycal considering the sterically hindered $Ir[P(OPh)_3]$-glycal π-complex (Table 1, entry 5). As summarized in Table 1, $[Ir(COE)_2Cl]_2$ afforded the desired glycosylated product **3a**, but lower yield (33%) was attained. With the optimized conditions in hand, a range of nucleophilic acceptors was reacted with 3,4,6-tri-*O*-benzyl-D-galactal (**1a**) to investigate the donor scope of the Ir-catalyzed hydro-alkoxy addition (Fig. 1). A large variety of substituents on the glycosyl acceptors were well tolerated, constituting commonly used carbohydrate protecting groups, *e.g.* acetal, ester, ether, and phthalimide, and all the reactions afforded desired 2-deoxy glycosides in a yield range of 47–85% with α-stereoselectivity. It is worth noting that in the case of **3b** (α : β = >5 : 1), **3c** (α : β = 17 : 1) and **3e** (α : β = >14 : 1) β-isomers were identified from ^{1}H NMR but with a favourable α-stereoselectivity and good yield (67%, 85% and 79% respectively, Fig. 1). The reaction proceeded equally well with secondary hydroxyl groups positioned at variable positions on the pyranose ring of different carbohydrates including glucose (**2h**, **2i** and **2j**, see the ESI†), glucosamine (**2k**, see the ESI†), mannose (**2f** and **2g**, see the ESI†), and fructose (**2d**, see the ESI†). To our satisfaction, the transformation provided the desired glycosides in moderate to high yield while maintaining excellent α-stereoselectivity. The reported method enabled glycosylations of the sterically hindered alcohols (**2f** and **2r**, see the ESI†) that gave the corresponding products (**3f** and **3l**, respectively, Fig. 1) in high yields with α-stereoselectivity upon isolation. We then assessed the reaction with an array of glycal donors embedded with a variety of ether and ester protections and satisfactorily all the tested donors were quite compatible and afforded desired α-glycosides in good to excellent yields (summarized in Table 2). It is important to note that when we carried out the reaction with conformationally unrestricted glucal **1k**, we obtained more

Table 1 Optimization of the Ir(I)-catalyzed glycosylation for the synthesis of 2-deoxy glycosides with glycal **1a** and model acceptor **2a**[a]

Entry	Catalyst (mol%)	Ag-Salt (mol%)	Solvent	Yield	α : β[b]
1	$[Ir(COD)Cl]_2$ (3.5)	—	DCM	—	NA
2	$[Ir(COD)Cl]_2$ (2.5)	AgOTf (5)	DCM	30%	1 : 0
3	$[Ir(COD)Cl]_2$ (3.5)	AgOTf (7)	DCM	45%	1 : 0
4	$[Ir(COD)Cl]_2$ (3.5)	AgOTf (10.5)	DCM	77%	1 : 0
5[c]	$[Ir(COD)Cl]_2$ (3.5)	AgOTf (10.5)	DCM	—	NA
6	—	AgOTf (10.5)	DCM	29%	1 : 0
7	$[Ir(COD)Cl]_2$ (3.5)	AgOTf (10.5)	MeCN	27%	15 : 1
8	$[Ir(COD)Cl]_2$ (3.5)	AgOTf (10.5)	Toluene	41%	1 : 0
9	$[Ir(COD)Cl]_2$ (3.5)	AgOTf (10.5)	DCE	52%	1 : 0
10	$[Ir(COD)Cl]_2$ (3.5)	AgOTf (10.5)	$CHCl_3$	66%	1 : 0
11	$[Ir(COD)Cl]_2$ (3.5)	AgOTf (10.5)	1,4-Dioxane	—	NA
12	$[Ir(COD)Cl]_2$ (3.5)	$AgSbF_6$ (10.5)	DCM	23%	1 : 0
13	$[Ir(COD)Cl]_2$ (3.5)	$AgBF_4$ (10.5)	DCM	40%	1 : 0
14	$[Ir(COD)Cl]_2$ (3.5)	$AgPF_6$ (10.5)	DCM	—	NA
15	$[Ir(COE)_2Cl]_2$ (3.5)	AgOTf (10.5)	DCM	33%	1 : 0

[a] All the reactions were carried out with 0.15 mmol **1a** and 0.1 mmol **2a**. [b] Stereoselectivity was determined by crude ^{1}H NMR. [c] $P(OPh)_3$ was used as a ligand. Isolated yields.

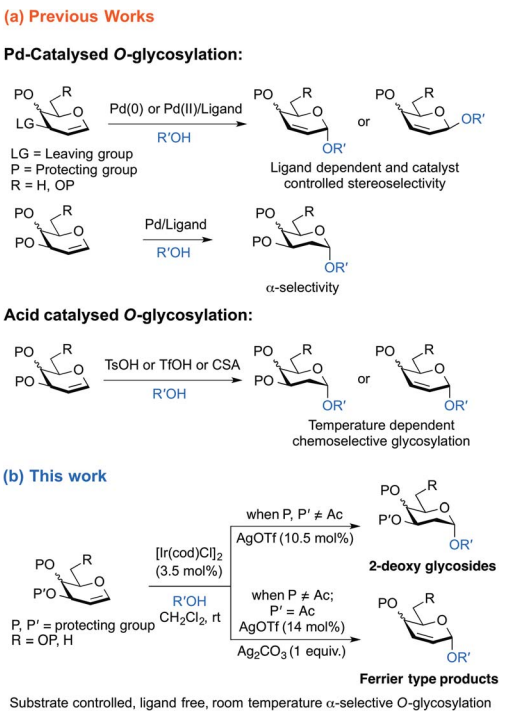

Scheme 1 (a) Recent development in stereoselective conversion of glycals to 2-deoxy glycosides and 2,3-unsaturated glycosides; (b) Ir(I)-catalyzed substrate controlled α stereoselective-*O*-glycosylation of glycals.

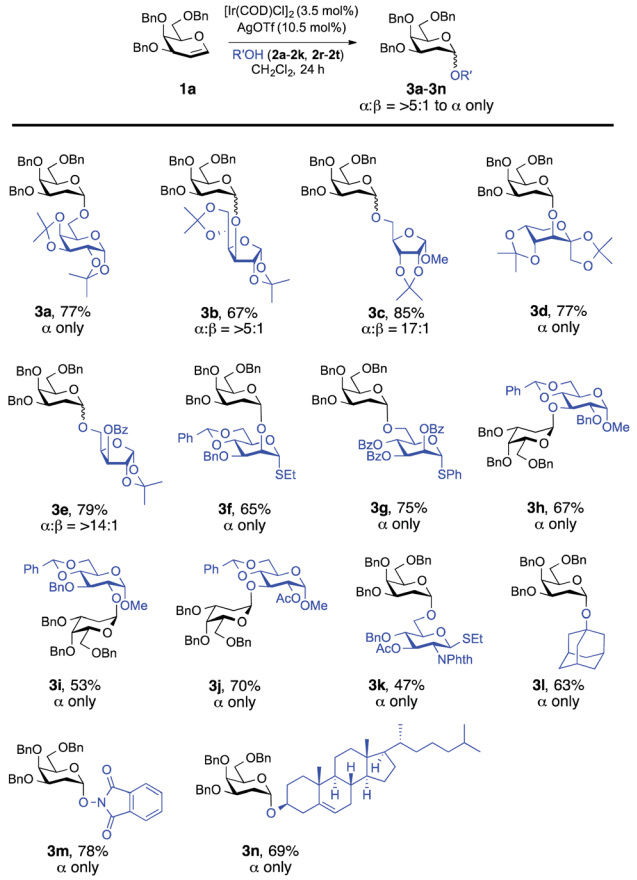

Fig. 1 Stereoselective α-*O*-glycosylation of **2a** with a range of glycosyl acceptors (**2a–2n**). Reactions were carried out under a N_2 atmosphere using 1.5 equiv. 3,4,6-tri-*O*-benzyl-D-galactal (**1a**), 1.0 equiv. of acceptor, 3.5 mol% $[Ir(COD)Cl]_2$, and 10.5 mol% AgOTf in dry CH_2Cl_2 for 24 h at rt. Stereoselectivity was determined by crude ^1H NMR. Isolated yields.

Ferrier product (71%, entry 10, Table 2) than 2-deoxy glycoside (8%), whereas we acquired only 2-deoxy glycoside with conformationally restricted glucal (**1j**, entry 9, Table 2) and rhamnal (**1l**). Thus, the formation of either glycosidic product greatly depends both on the stereochemistry and conformation of the protecting groups in the glycals.[3b,c]

We have shown that glycals bearing a poor leaving group at C3 reacted with alcohols to provide 2-deoxy-α-*O*-glycosides; thus we became intrigued about the possible outcome of repeating the same transformation on glycals with a good leaving group at the C3 position. We initiated our studies by employing 3-*O*-acetyl-4,6-di-*O*-allyl-D-glucal with 1,2:3,4-di-*O*-isopropylidene-α-D-galactopyranose (**2a**) and found that the optimal conditions (3.5 mol% $[Ir(COD)Cl]_2$, 14 mol% AgOTf, and 1 equiv. of Ag_2CO_3) worked just as effectively as they did for 2-deoxy-*O*-glycoside synthesis (entry 4, Table 3). We examined the effect of solvation and found that solvents like MeCN (39%, entry 6, Table 3) and DCE (34%, entry 8) constrained the desired product formation (Table 3). Toluene (entry 7, Table 3) and $CHCl_3$ (entry 9, Table 3) provided the product in 52% and 57% yield, respectively, but we attained the finest yield (73%) for the

Table 2 Reaction of glycals **1b–1i**, **1j–1k**, and **1l** with model glycoside acceptor **2a**[a]

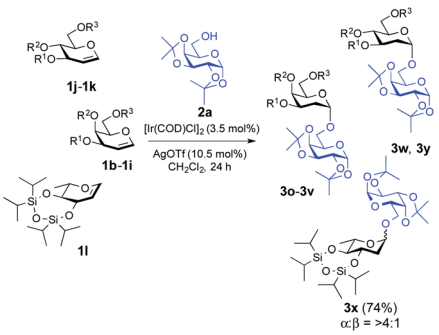

Entry	Donor	R^1	R^2	R^3	Product	Yield (%)	α : β
1	**1b**	Me	Me	Me	**3o**	83%	1 : 0
2	**1c**	Et	Et	Et	**3p**	78%	23 : 1
3	**1d**	Allyl	Allyl	Allyl	**3q**	82%	1 : 0
4	**1e**	TBDMS	TBDMS	TBDMS	**3r**	80%	1 : 0
5	**1f**	TBDMS	Ac	TBDMS	**3s**	76%	1 : 0
6	**1g**	Bn	Bn	TBDPS	**3t**	79%	10 : 1
7	**1h**	Bn	Bn	Ac	**3u**	86%	>30 : 1
8	**1i**	Bn	Ac	Bn	**3v**	81%	1 : 0
9	**1j**	$O[Si(iPr)_2]_2$		TBDPS	**3w**	78%	1 : 0
10[b]	**1k**	TBDMS	TBDMS	TBDMS	**3y**	8%	1 : 0

[a] All the reactions were carried out under a N_2 atmosphere using 1.5 equiv. glycosyl donors (**1b–1k**) and 1.0 equiv. acceptor (**2a**) in dry CH_2Cl_2 for 24 h. [b] **4r** obtained as a major product (71%). Stereoselectivity was determined by crude ^1H NMR. Isolated yields.

Table 3 Optimization of the Ir(I)-catalyzed glycosylation for the synthesis of 2, 3-unsaturated glycosides with glycal **1n** and model acceptor **2a**[a]

Entry	Catalyst (mol%)/Ag-salt (mol%)	Base	Solvent	Yield
1	$[Ir(cod)Cl]_2$ (2.5)/AgOTf (5)	Ag_2CO_3	DCM	23%
2	$[Ir(cod)Cl]_2$ (3.5)/AgOTf (7)	Ag_2CO_3	DCM	42%
3	$[Ir(cod)Cl]_2$ (3.5)/AgOTf (10.5)	Ag_2CO_3	DCM	66%
4	$[Ir(cod)Cl]_2$ (3.5)/AgOTf (14)	Ag_2CO_3	DCM	73%
5	AgOTf (14)	Ag_2CO_3	DCM	36%
6	$[Ir(cod)Cl]_2$ (3.5)/AgOTf (14)	Ag_2CO_3	MeCN	39%
7	$[Ir(cod)Cl]_2$ (3.5)/AgOTf (14)	Ag_2CO_3	Toluene	52%
8	$[Ir(cod)Cl]_2$ (3.5)/AgOTf (14)	Ag_2CO_3	DCE	34%
9	$[Ir(cod)Cl]_2$ (3.5)/AgOTf (14)	Ag_2CO_3	$CHCl_3$	57%
10	$[Ir(cod)Cl]_2$ (3.5)/AgOTf (14)	Cs_2CO_3	DCM	45%

[a] All the reactions were carried out with 0.15 mmol **1n**, 0.1 mmol **2a** and 1 mmol base for 48 h. For all entries we obtained exclusively α selectivity. Isolated yields.

allylic substitution reaction when we carried out the reaction in CH_2Cl_2 (entry 4, Table 3). After optimizing the parameters, we turned our attention to exploring the feasibility of the donor scope and we found that our reaction conditions worked well with the set of commonly used carbohydrate protecting groups with 61–79% yield (Table 4). The protecting groups at the C4 and C6 positions in the glycosyl donors had a pronounced effect on the yields and outcome of the reactions. Specifically, keeping

Table 4 Ferrier type glycosylation of various glycals **1n–1r** with glycoside acceptor **2a**[a]

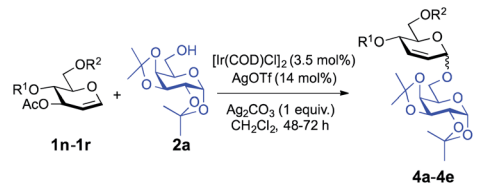

Entry	Donor	R^1	R^2	Product	Yield (%)	α : β[b]
1	**1n**	Allyl	Allyl	**4a**	73%	1 : 0
2	**1o**	Et	Et	**4b**	61%	>8 : 1
3	**1p**	Bn	Bn	**4c**	79%	9 : 1
4	**1q**	PMB	PMB	**4d**	75%	>13 : 2
5	**1r**	PX	PX	**4e**	70%	19 : 1

[a] All the reactions were carried out under a N_2 atmosphere using 1.5 equiv. glycosyl donors (**1n–1r**) and 1.0 equiv. acceptor (**2a**) in dry CH_2Cl_2 for 48–72 h. [b] Stereoselectivity was determined by crude ^{1}H NMR. Isolated yields. PX = *p*-xylyl.

m-nitrobenzyl protection on the donor (**1s**, see the ESI†) didn't afford the desired product. Taking the strong electron-withdrawing nature of *m*-nitro group into account, we suggest that it disrupts the positively charged π-allylic system, thus leading the reaction to fail. We observed a similar outcome in the case of peracetylated glucal, perhaps due to the same sort of electron-withdrawing nature of the acetyl group. The reported method also failed to provide the desired glycoside with 4,6-*O*-*p*-methoxybenzylidene-3-*O*-acetyl-D-glucal (**1t**, see the ESI†) signifying the requirement of conformationally flexible C4 and C6 protecting groups.

To evaluate the synthetic applicability of this method, we used a series of glycosyl acceptors for the Ferrier-type nucleophilic substitution reactions (Fig. 2). To our delight, the versatility proved to be highly efficient since glycosylations proceeded smoothly to furnish the desired glycosides in yields of 54–79% and with high α-selectivity (>6 : 1 α : β to α only, Fig. 2). Notably, sterically hindered alcohols **2l** and **2p** (see the ESI†) underwent coupling stereoselectively to give **4h** (α : β, >14 : 1) and **4l** (α : β, >13 : 1) in 54% and 76% yield, respectively. Glycosyl acceptors containing benzoate and phthalimide protecting groups (**2l**, **2m** and **2n**, see the ESI†) are also well tolerated by this procedure, with desired disaccharides **4h**, **4i** (α : β, >8 : 1) and **4j** (α only) generated in moderate to good yields (54%, 72%, and 61%, respectively, Fig. 2).

Moreover, this method is quite amenable with several primary and secondary alcohols, yielding the desired disaccharides with high efficiency and good α-selectivity. To interpret the mechanism of this reaction, we carried out DFT study. We proposed that to start the catalytic cycle, $[Ir(COD)Cl]_2$ first reacts with AgOTf to generate the active species $[Ir(COD)OTf]_2$ (Fig. 3).[18] The dimer complex then dissociates into two transient monomeric Ir(COD)OTf complexes (see the ESI†), which in turn coordinate to the glycal. We rationalize that for the 3,4,6-tri-*O*-benzyl glycal donor **1a**, the iridium metal center coordinates to

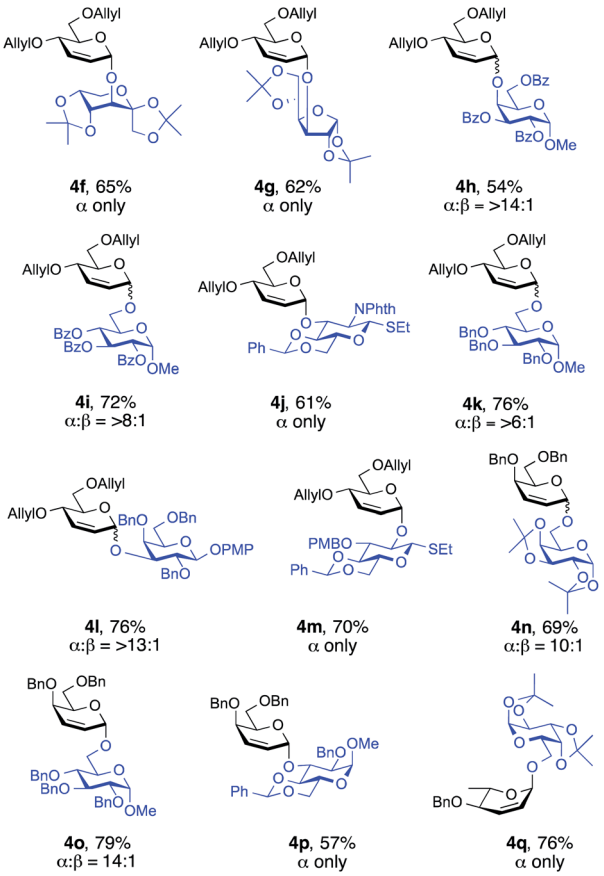

Fig. 2 α-Selective Ferrier type *O*-glycosylation of **1n**, **1u** and **1v** with a variety of glycosyl acceptors. Reactions were carried out under a N_2 atmosphere using 1.5 equiv. glycosyl donor (**1**), 1.0 equiv. of acceptor (**2**), 3.5 mol% $[Ir(COD)Cl]_2$, 14.0 mol% AgOTf, and 1.0 equiv. of Ag_2CO_3 in dry CH_2Cl_2 for 48–72 h at rt. Stereoselectivity was determined by crude ^{1}H NMR. Isolated yields.

the olefinic C1 and C2 carbon to form stable η^2 π-allyl intermediates, while for the 3-*O*-acetyl-4,6-di-*O*-benzyl-D-galactal donor **1u**, which carries a better leaving group at the 3-position, the Ir(COD)OTf species first coordinates to C1 and C2 to form η^2 π-allyl intermediates, and then, upon dissociation of the triflate anion from the metal center, the metal center further coordinates with C3 to form an η^3 π-allyl complex, expelling the 3-acetyl substituent as an acetate anion, which may then coordinate to the metal center as a free ligand (Fig. 3). Importantly, Ir(COD)OTf can coordinate to the glycal at either face of the pyranose ring, with one face preferred over another due to steric and electronic factors. The relative stability of possible intermediate species, as well as the activation energy of the following nucleophilic attack on the iridium coordinated glycal intermediate by the acceptor, determines the favored reaction routes and has a major influence on the stereochemical outcome of the glycosylation reaction. Upon formation of the major iridium-glycal π-allyl complex intermediates, anomeric carbon on the glycal becomes activated, and we hypothesize that the acceptor coordinates to the iridium center in the metal-glycal complex first (see the ESI† for a detailed discussion), and then attacks

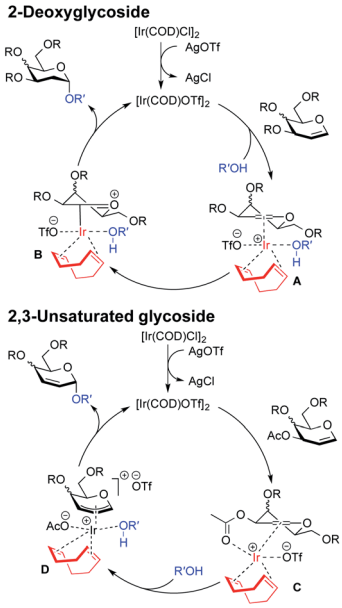

Fig. 3 Schematic representation of the proposed mechanism giving rise to 2-deoxy-α-glycoside and 2,3-unsaturated-α-glycoside arising from Ir(I)-catalyzed *O*-glycosylation.

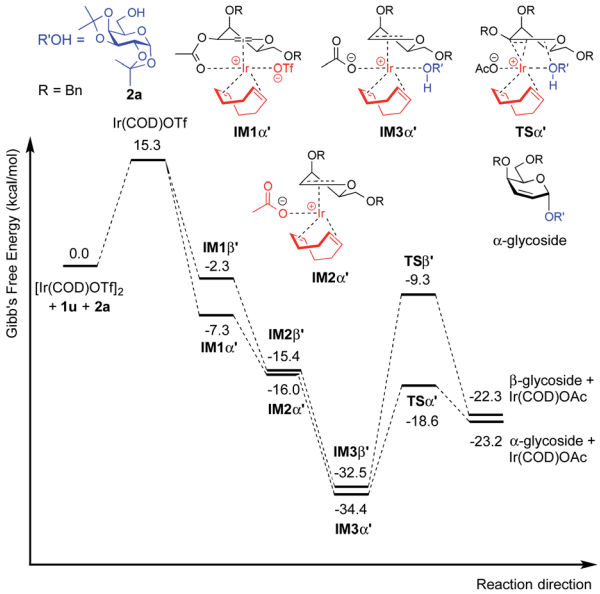

Fig. 5 Free energy profile for the catalytic cycle of iridium catalyzed glycosylation of 3-*O*-acetyl-4,6-di-*O*-benzyl galactal (**1u**) with model acceptor **2a**.

the adjacent anomeric carbon in a *syn*-addition manner, leading to the formation of corresponding 2-deoxy or 2,3-unsaturated glycosides, while regenerating the catalytic complex (Fig. 3). DFT computed energetic profiles of important intermediates and transition states are shown in Fig. 4 and 5.

For galactal **1a**, intermediates arising from η^2 π-allyl coordination of Ir(COD)OTf to the glycal donor from both faces (**IM1α** and **IM1β**) are energetically similar (Fig. 4). The stronger steric repulsion in β-face coordinated **IM1β** might be compensated by the stabilization of hydrophobic interactions between the C3 benzyl group and the cyclohexadiene group in the complex. Contrarily, for galactal **1u**, the η^2 π-allyl complex with Ir(COD)OTf from the α-face (**IM1α′**) is sizably more stable than the β-face counterpart **IM1β′** (Fig. 5), probably due to the difficulty of covalently linked C3 acetyl to interact with the iridium metal center and stabilize the intermediate complex. This explanation is corroborated by the results that the η^3 π-allyl coordinated complexes **IM2α′** and **IM2β′**, both having the dissociated acetate ligand coordinating to the iridium metal center, are rather similar in energy level.

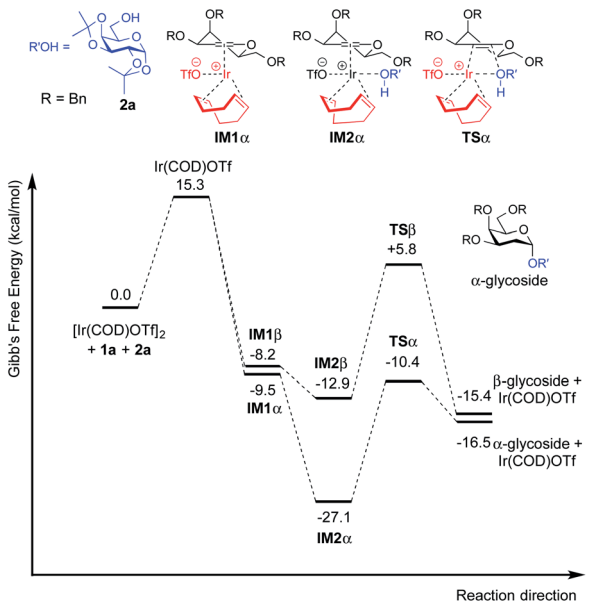

Fig. 4 Free energy profile for the catalytic cycle of Ir(I)-catalyzed glycosylation of 3,4,6-tri-*O*-benzyl galactal (**1a**) with model acceptor **2a**.

Although the metal coordinated intermediates without the acceptor coordinating to the metal center show minor facial preference for both **1a** and **1u**, for the acceptor coordinated intermediates arising from **1a**, the computation results suggest an appreciable α-face preference. The higher energy level of the β-face coordinated intermediates with the acceptor coordinated to the metal center can be mainly attributed to the steric crowding of the β-face intermediate **IM2β** (see the ESI†). The steric repulsion effect is significantly less pronounced in the **IM3β′** arising from C3 acetyl galactal **1u**, which, without the absence of a bulky C3 benzyl substituent, leaves the β-face coordinated Ir(COD) group a larger space for accommodating the additional coordination to the acceptor (see the ESI†).

For both **1a** and **1u**, activation energy of the transition state of the nucleophilic attack step shows a strong α-face preference. For all TSs (transition states) arising from nucleophilic attack of the acceptor on the glycal donor, the iridium metal center dissociates from C1 yet remains largely coordinated to C2 (Fig. 6). Similar to the scenario of the acceptor coordinated intermediates, the α-face preference of the TS arising from nucleophilic attack on iridium-coordinated **1a** mainly results

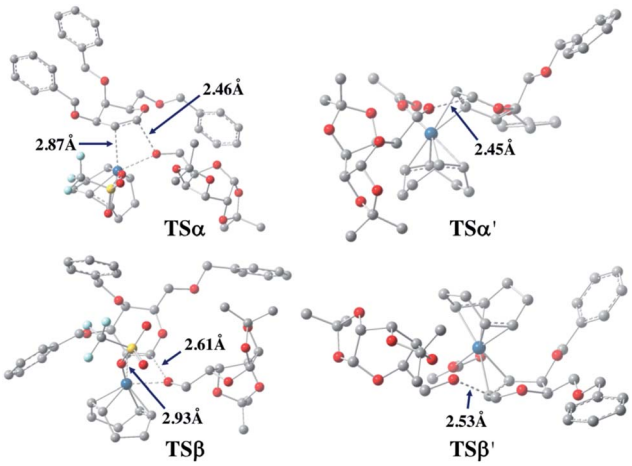

Fig. 6 Optimized transition state structures arising from nucleophilic attack of **2a** on **1a** (left) and **1u** (right).

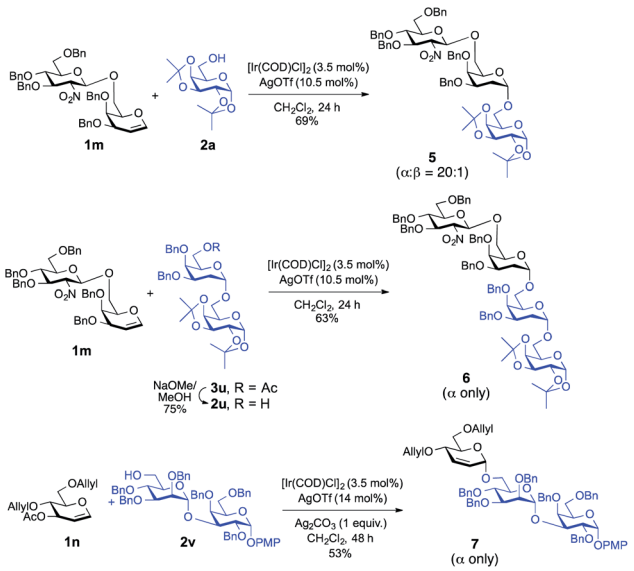

Scheme 2 Ir(I)-Catalyzed α-stereoselective-*O*-glycosylation for the synthesis of model trisaccharides and tetrasaccharides.

from steric crowding of the β-face TS, while for the TSs arising from nucleophilic attack on iridium-coordinated **1u**, the α-preference is possibly due to a combination of steric factors and the anomeric effect.

The DFT computation results suggest that both the reaction routes leading to α-products are kinetically favored. The reaction proceeds through a directing mechanism, with α-face intermediates generally more stable than the β-counterparts along the reaction routes, and the energy of the transition state for nucleophilic attack from the α-face significantly lower than the energy of the TS of the β-face nucleophilic attack, which likely arises from a combination of the unfavorable steric interactions between the 3-substituents and the metal complex in the TSs and the anomeric effect. The theoretically inferred coordination of the acceptor to the iridium is further corroborated by ^{1}H NMR investigations, in which addition of the iridium catalyst (equimolar w.r.t. **2a**) to the acceptor in CD_2Cl_2 results in a pronounced downfield shifting of the hydroxy proton from 1.714 ppm to 2.231 ppm, indicating probable coordination between the OH group and the Ir(I) center. The theoretically proposed coordination of iridium metal to the glycal substrate in the catalytic cycle is also supported by ^{1}H NMR experiments, in which addition of the iridium catalyst to a solution of **1a** in CD_2Cl_2 resulted in an appreciable downfield shifting of the alkene protons from 6.333 ppm and 4.843 ppm to 6.613 ppm and 5.007 ppm, respectively, indicating probable coordination between the glycal π-system and the iridium center. The downfield shifting of alkene protons upon coordination to the iridium metal center is rationalized by computation of the partial charges of the C2 atom in both the free **1a** substrate and the stable intermediate arising from **1a** complexed to the iridium metal center at the α face, with alcohol coordinated to the iridium. The computed partial charge of C2 in the coordinated intermediate is more positive (−0.147) with respect to the partial charge of C2 in free **1a** (−0.168), indicating a chemical environment of lower electron density for alkene protons upon coordination. The computed partial charge of C1 in the same intermediate is also significantly more positive (0.230) with respect to C1 in free **1a** (0.187), agreeing with our hypothesis that coordination of the glycal to the iridium catalyst enhances the electrophilicity of the donor anomeric center and facilitates the nucleophilic attack by alcohol under mild conditions.

To demonstrate the applicability of this newly developed methodology, synthesis of oligosaccharides has been conducted. As shown in Scheme 2, disaccharide donor **1m** was reacted with the model acceptor **2a**, which afforded the corresponding trisaccharide, **5**, in 69% yield with desirable high α-selectivity ($\alpha : \beta = 20 : 1$). Then previously synthesized disaccharide **3u** was subjected for selective deacetylation[19] using NaOMe in MeOH which afforded acceptor **2u** in 75% yield.

On a similar note, glycosylation of the same disaccharide donor **1m** with glycosyl acceptor **2u** proceeded smoothly to give the corresponding tetrasaccharide, **6**, in 63% yield with an absolute α-stereoselectivity. Finally, in a separate experiment, we employed the Ir(I)-catalyst successfully to synthesize 2,3-unsaturated-*O*-glycoside containing trisaccharide **7** with complete α-selectivity from monosaccharide donor **1n** and disaccharide acceptor **2v** in a decent yield (53%), which demonstrates the practical utility of this method in the synthesis of higher analogue glycans.

Conclusion

To summarize, we have demonstrated two concurrent Ir(I)-catalyzed glycosylation events that can be independently adjusted by exploiting a substrate-controlled approach on the glycal donors. The Ir(I)-catalyzed glycosylation reaction of glycal donors with an armed group at C3 affords 2-deoxy-*O*-glycoside, while glycosylation of a C3-acetyl glycal donor affords 2,3-unsaturated-*O*-glycoside. For both types of the Ir(I)-catalyzed

glycosylation, we optimized the reaction conditions with α stereoselectivity, and then the generality of the Ir(I)-catalyzed glycosylation was shown in over 40 examples featuring a range of glycal donors and acceptors bedecked with commonly used protecting groups. Our results confirm that the Ir(I)-catalyzed alcohol glycosylation reaction can be feasibly performed under mild conditions, requiring a catalytic amount of the Ir(I)-catalyst for activation of glycal donors. The mechanism accounting for the α-stereoselectivity of the Ir(I)-catalyzed-glycosylation by glycal donors was investigated with DFT calculations. We further demonstrated that our Ir(I)-catalyzed glycosylation methods can be implemented for the construction of trisaccharides and tetrasaccharides, and presumably oligosaccharides, enabling facile access to biologically important oligosaccharides comprising 2-deoxy-sugar structures connected by α-glycosidic linkages.

Conflicts of interest

The authors declare no competing financial interests.

Acknowledgements

K. B. Pal and T.-P. Loh thank Northwestern Polytechnical University for their financial support. We thank the Nanyang Technological University (RG9/20) and National Research Foundation (NRF2016NRF-NSFC002-005), Singapore for their financial support.

Notes and references

1 (*a*) R. M. De Lederkremer and C. Marino, *Adv. Carbohydr. Chem. Biochem.*, 2008, **61**, 143–216; (*b*) E. K. McCranie and B. O. Bachmann, *Nat. Prod. Rep.*, 2014, **31**, 1026–1042.

2 (*a*) H. M. Zuurmond, P. A. M. van der Klein, G. A. van der Marel and J. H. van Boom, *Tetrahedron*, 1993, **49**, 6501–6514; (*b*) J. P. Issa, D. Lloyd, E. Steliotes and C. S. Bennett, *Org. Lett.*, 2013, **15**, 4170–4173; (*c*) E. I. Balmond, D. Benito-Alifonso, D. M. Coe, R. W. Alder, E. M. McGarrigle and M. C. Galan, *Angew. Chem., Int. Ed.*, 2014, **53**, 8190–8194; (*d*) J. P. Yasomanee and A. V. Demchenko, *Angew. Chem., Int. Ed.*, 2014, **53**, 10453–10456; (*e*) J. P. Issa and C. S. Bennett, *J. Am. Chem. Soc.*, 2014, **136**, 5740–5744; (*f*) J. H. Ruei, P. Venukumar, A. B. Ingle and K. K. Mong, *Chem. Commun.*, 2015, **51**, 5394–5397; (*g*) J. Wang, C. Deng, Q. Zhang and Y. Chai, *Org. Lett.*, 2019, **21**, 1103–1107.

3 (*a*) A. Sau, C. Palo-Nieto and M. C. Galan, *J. Org. Chem.*, 2019, **84**, 2415–2424; (*b*) M. B. Tatina, Z. Moussa, M. Xia and Z. M. A. Judeh, *Chem. Commun.*, 2019, **55**, 12204–12207; (*c*) M. B. Tatina, X. Mengxin, R. Peilin and Z. M. A. Judeh, *Beilstein J. Org. Chem.*, 2019, **15**, 1275–1280.

4 (*a*) M. J. McKay and H. M. Nguyen, *ACS Catal.*, 2012, **2**, 1563–1595; (*b*) X. Li and J. Zhu, *Eur. J. Org. Chem.*, 2016, 4724–4767; (*c*) G. Zhao and T. Wang, *Angew. Chem., Int. Ed.*, 2018, **57**, 6120–6124.

5 (*a*) B. D. Sherry, R. N. Loy and F. D. Toste, *J. Am. Chem. Soc.*, 2004, **126**, 4510–4511; (*b*) C. S. Bennett and M. C. Galan, *Chem. Rev.*, 2018, **118**, 7931–7985; (*c*) N. Ibrahim, M. Alami and S. Messaoudi, *Asian J. Org. Chem.*, 2018, **7**, 2026–2038; (*d*) Q. Wang, S. An, Z. Deng, W. Zhu, Z. Huang, G. He and G. Chen, *Nat. Catal.*, 2019, **2**, 793–800; (*e*) N. Jiang, Z. Wu, Y. Dong, X. Xu, X. Liu and J. Zhang, *Curr. Org. Chem.*, 2020, **24**, 184–199.

6 (*a*) S. Xiang, J.-X. He, Y. J. Tan and X.-W. Liu, *J. Org. Chem.*, 2014, **79**, 11473–11482; (*b*) S. Xiang, K. L. M. Hoang, J.-X. He, Y. J. Tan and X.-W. Liu, *Angew. Chem., Int. Ed.*, 2015, **54**, 604–607; (*c*) L. Ji, S. Xiang, W. L. Leng, K. L. M. Hoang and X.-W. Liu, *Org. Lett.*, 2015, **17**, 1357–1360; (*d*) W. L. Leng, H. Liao, H. Yao, Z.-E. Ang, S. Xiang and X.-W. Liu, *Org. Lett.*, 2017, **19**, 416–419.

7 (*a*) B. P. Schuff, G. J. Mercer and H. M. Nguyen, *Org. Lett.*, 2007, **9**, 3173–3176; (*b*) H. Yao, S. Zhang, W. L. Leng, M. L. Leow, S. Xiang, J.-X. He, H. Liao, K. L. M. Hoang and X.-W. Liu, *ACS Catal.*, 2017, **7**, 5456–5460.

8 (*a*) H. Kim, H. Men and C. Lee, *J. Am. Chem. Soc.*, 2004, **126**, 1336–1337; (*b*) J. Yang, C. Cooper-Vanosdell, E. A. Mensah and H. M. Nguyen, *J. Org. Chem.*, 2008, **73**, 794–800; (*c*) E. A. Mensah, J. M. Azzarelli and H. M. Nguyen, *J. Org. Chem.*, 2009, **74**, 1650–1657; (*d*) A. Sau, R. Williams, C. Palo-Nieto, A. Franconetti, S. Medina and M. C. Galan, *Angew. Chem., Int. Ed.*, 2017, **56**, 3640–3644; (*e*) A. Sau and M. C. Galan, *Org. Lett.*, 2017, **19**, 2857–2860.

9 (*a*) R. Takeuchi and M. Kashio, *J. Am. Chem. Soc.*, 1998, **120**, 8647–8655; (*b*) T. Graening and J. F. Hartwig, *J. Am. Chem. Soc.*, 2005, **127**, 17192–17193; (*c*) N. Nomura, S. Komiyama, H. Kasugai and M. Saba, *J. Am. Chem. Soc.*, 2008, **130**, 812–814; (*d*) S. Pan and T. Shibata, *ACS Catal.*, 2013, **3**, 704–712; (*e*) J. Qu and G. Helmchen, *Acc. Chem. Res.*, 2017, **50**, 2539–2555; (*f*) K. Spielmann, G. Niel, R. M. D. Figueiredo and J.-M. Campagne, *Chem. Soc. Rev.*, 2018, **47**, 1159–1173.

10 (*a*) E. Genin, S. Antoniotti, V. Michelet and J.-P. Genêt, *Angew. Chem., Int. Ed.*, 2005, **44**, 4949–4953; (*b*) X. Li, A. R. Chianese, T. Vogel and R. H. Crabtree, *Org. Lett.*, 2005, **7**, 5437–5440; (*c*) J. P. Roberts and C. Lee, *Org. Lett.*, 2005, **7**, 2679–2682; (*d*) T. Fjermestad, J. H. H. Ho, S. A. Macgregor, B. A. Messerle and D. Tuna, *Organometallics*, 2011, **30**, 618–626; (*e*) C. S. Sevov and J. F. Hartwig, *J. Am. Chem. Soc.*, 2013, **135**, 2116–2119; (*f*) C. S. Sevov and J. F. Hartwig, *J. Am. Chem. Soc.*, 2013, **135**, 9303–9306; (*g*) M. C. Haibach, C. Guan, D. Y. Wang, B. Li, N. Lease, A. M. Steffens, K. Krogh-Jespersen and A. S. Goldman, *J. Am. Chem. Soc.*, 2013, **135**, 15062–15070; (*h*) M. Nagamoto and T. Nishimura, *Chem. Commun.*, 2015, **51**, 13466–13469; (*i*) Y. Chen, Z.-X. Wang, Q. Li, L.-J. Xu and B.-J. Li, *Org. Chem. Front.*, 2018, **5**, 1815–1819.

11 (*a*) E. A. Mensah and H. M. Nguyen, *J. Am. Chem. Soc.*, 2009, **131**, 8778–8780; (*b*) E. A. Mensah, F. Yu and H. M. Nguyen, *J. Am. Chem. Soc.*, 2010, **132**, 14288–14302.

12 (*a*) S. Hotha and S. Kashyap, *J. Am. Chem. Soc.*, 2006, **128**, 9620–9621; (*b*) A. S. K. Hashmi, *Chem. Rev.*, 2007, **107**, 3180–3211; (*c*) C. Zhu, P. Tang and B. Yu, *J. Am. Chem. Soc.*, 2008, **130**, 5872–5873; (*d*) Y. Li, Y. Yang, Y. Liu, C. Zhu, Y. Yang and B. Yu, *Chem.–Eur. J.*, 2010, **16**, 1871–1882; (*e*) Y. Li and B. Yu, *Chem. Commun.*, 2010, **46**, 6060–

6062; (*f*) C. Palo-Nieto, A. Sau and M. C. Galan, *J. Am. Chem. Soc.*, 2017, **139**, 14041–14044.

13 (*a*) R. Benhaddou, S. Czernecki and G. Ville, *J. Org. Chem.*, 1992, **57**, 4612–4616; (*b*) M. Sakai, H. Hayashi and N. Miyaura, *Organometallics*, 1997, **16**, 4229–4231; (*c*) J. Ramnauth, O. Poulin, S. S. Bratovanov, S. Rakhit and S. P. Maddaford, *Org. Lett.*, 2001, **3**, 2571–2573.

14 B. D. Sherry, R. N. Loy and F. D. Toste, *J. Am. Chem. Soc.*, 2004, **126**, 4510–4511.

15 (*a*) S. Suda and T. Mukaiyama, *Chem. Lett.*, 1991, 431–434; (*b*) T. Mukaiyama, M. Yamada, S. Suda, Y. Yokomizo and S. Kobayashi, *Chem. Lett.*, 1992, 1401–1404; (*c*) M. Pfaffe and R. Mahrwald, *Org. Lett.*, 2012, **14**, 792–795.

16 (*a*) M. M. Mukherjee, N. Basu and R. Ghosh, *RSC Adv.*, 2016, **6**, 105589–105606; (*b*) A. Stévenin, F.-D. Boyer and J.-M. Beau, *Eur. J. Org. Chem.*, 2012, 1699–1702; (*c*) A. Xolin, A. Stevenin, M. Pucheault, S. Norsikian, F.-D. Boyer and J.-M. Beau, *Org. Chem. Front.*, 2014, **1**, 992–1000; (*d*) L. Adak, S. Kawamura, G. Toma, T. Takenaka, K. Isozaki, H. Takaya, A. Orita, H. C. Li, T. K. M. Shing and M. Nakamura, *J. Am. Chem. Soc.*, 2017, **139**, 10693–10701.

17 K. Sakamoto, M. Nagai, Y. Ebe, H. Yorimitsu and T. Nishimura, *ACS Catal.*, 2019, **9**, 1347–1352.

18 (*a*) J. F. Hartwig and L. M. Stanley, *Acc. Chem. Res.*, 2010, **43**, 1461–1475; (*b*) B. Zhu, X. Cui, C. Pi, D. Chen and Y. Wu, *Adv. Synth. Catal.*, 2016, **358**, 326–332; (*c*) X. Xiao, C. Hou, Z. Zhang, Z. Ke, J. Lan, H. Jiang and W. Zeng, *Angew. Chem., Int. Ed.*, 2016, **55**, 11897–11901; (*d*) Y. Li, F. Wang, S. Yu and X. Li, *Adv. Synth. Catal.*, 2016, **358**, 880–886; (*e*) H. Hou, Y. Zhao, S. Sheng and J. Chen, *Adv. Synth. Catal.*, 2019, **361**, 4393–4398.

19 G. Zemplén, *Ber. Dtsch. Chem. Ges.*, 1926, **59**, 1254–1266.